



# Investigating and Ranking Blasting Patterns to Reduce Ground Vibration using Soft Computing Approaches and MCDM Technique

D. Mohammadi<sup>1</sup>, R. Mikaeil<sup>2\*</sup> and J. Abdollahei Sharif<sup>3</sup>

*1-Department of Mining, Ahar Branch, Islamic Azad University Ahar, Ahar, Iran  
2-Department of Mining engineering, Urmia University of Technology, Urmia, Iran  
3-Department of Mining engineering, Urmia University, Urmia, Iran*

Received 7 March 2020; received in revised form 15 June 2020; accepted 28 June 2020

## Keywords

*Blasting*  
*Ground Vibration*  
*Clustering*  
*ICA, K-means*  
*MCDM*  
*TOPSIS*

## Abstract

The blasting method is one of the most important operations in most open-pit mines that has a priority over the other mechanical excavation methods due to its cost-effectiveness and flexibility in operation. However, the blasting operation, especially in surface mines, imposes some environmental problems including the ground vibration as one of the most important ones. In this work, an evaluation system is provided to study and select the best blasting pattern in order to reduce the ground vibration as one of the hazards in using the blasting method. In this work, 45 blasting patterns used for the Sungun copper mine are studied and evaluated to help determine the most suitable and optimum blasting pattern for reducing the ground vibration. Additionally, due to the lack of certainty in the nature of ground and the analyses relating to this drilling system, in the first step, a combination of the imperialist competitive algorithm and k-means algorithm is used for clustering the measured data. In the second step, one of the multi-criteria decision-making methods, namely TOPSIS (Technique for Order Performance by Similarity to Ideal Solution), is used for the final ranking. Finally, after evaluating and ranking the studied patterns, the blasting pattern No. 27 is selected. This pattern is used with the properties including a hole diameter of 16.5 cm, number of holes of 13, spacing of 4 m, burden of 3 m, and ammonium nitrate fuel oil of 1100 Kg as the most appropriate blasting pattern leading to the minimum ground vibration and reduction of damages to the environment and structures constructed around the mine.

## 1. Introduction

The blasting process is a combination of different knowledge areas such as chemistry, physics, and thermodynamics, and one of the most common and easiest excavation methods in most of the large open-pit mines. Although this process has many advantages, the environmental problems such as fly rock, back-break, grinding, and ground vibration are some disadvantages of using this excavation method affecting the environment and the surrounding areas of open-pit mines. Various studies have been conducted to determine the prediction models and the blast-induced problems (Monjezi et al., 2013; Armaghani et al., 2015; Hasanipanah et al., 2015; Monjezi et al., 2016; Zhang et al., 2019; Shang et al., 2019; Nguyen

2019). In a study on the blasting process conducted by Singh and Singh (2005), it was found that only about 20-30% of the blasting energy was spent for the rock breakage, and the rest of the energy released from blasting was wasted in the forms of air blast, fly rock, ground vibration, and back-break, leading to environmental problems. In the study of Faradonbeh and Monjezi (2017), using the gene expression programming and the cuckoo optimization algorithm, the ground vibration phenomenon was predicted and minimized. The optimized results obtained from this study showed that the developed model could provide a higher performance capacity to reduce the ground vibration values. In a study conducted by

✉ Corresponding author: [Reza.mikaeil@uut.ac.ir](mailto:Reza.mikaeil@uut.ac.ir) (R. Mikaeil).

Shahnazar et al. (2017) using the PSO-ANFIS hybrid algorithm, a prediction model for ground vibration resulting from blasting was investigated. In their study, the particle swarm optimization (PSO) algorithm was used for the adaptive neuro-fuzzy inference system training, and the proposed model was provided using the data collected from 81 blasting operations in the Pengerang quarry. Finally, using the results obtained from these analyses, an advanced method with a high prediction ability of ground vibration was provided. In a research work conducted by Yari et al. (2017), an advanced evaluation system was presented for determining the most appropriate blasting pattern to increase the production productivity. The multi-attribute decision-making method was used for evaluating and ranking 29 blasting patterns. Finally, based on the results obtained, a blasting pattern with the highest production rate was determined. In another study conducted by Hasanipanah et al. (2017) for predicting the ground vibration of the blasting using a data collection of 80 blasts, the ground vibration phenomenon resulting from this excavation method was evaluated and an advanced method was proposed. In their analyses, the PSO algorithm was used, which, based on the results obtained, it was determined that the applicability of the PSO power model was more efficient compared to the other analysis models used in this study including the linear PSO, MLR, and USBM equations. In the study of Fouladgar et al. (2017) based on the results of blasts in the Miduk copper mine, an advanced model was presented using a novel swarm intelligence algorithm based on the cuckoo search for predicting the peak particle velocity in order to describe and evaluate the ground vibration phenomenon and the results obtained from this model were compared with the results obtained from the empirical relations. At last, comparison of results showed the superiority of the cuckoo search algorithm in the prediction of the peak particle velocity. In another study conducted by Armaghani et al. (2018), several advanced models using the imperialist competitive algorithm and empirical equations were applied to study the peak particle velocity as the descriptor of ground vibration phenomenon. Furthermore, the data obtained from 73 blasting patterns was used in these modellings. The results obtained showed the superiority of the advanced models based on the imperialist competitive algorithm over the empirical relations. In the study of Arthur et al. (2019), a novel approach was proposed to predict the blast-induced ground vibration. The Gaussian process regression

approach was used and 70 blasting operations were investigated. The results clearly showed the superiority of the proposed Gaussian process regression model in comparison with the other standard predictive techniques. In the study of Azimi et al. (2019), using the hybrid genetic algorithm optimized artificial neural network, the empirical predictors and neuro-fuzzy inference system, the ground vibration phenomenon was evaluated and studied. Their results showed that GA-ANN had a better ability in evaluating the ground vibration. In a study by Ataei & Baydokhti (2019), the repeated blasting effect on the surrounding rock weakness was studied using an experimental research work. The results obtained showed that weakness intensity in the second blasting round was increased compared to the first blasting result. In the study of Norouzi Masir et al. (2020), the risk assessment of fly rock in surface mines was investigated using the fuzzy fault tree analysis (FFTA)-multi-criteria decision-making (MCDM) methods.

Considering the literature review, some studies have been conducted using the developed models, and in spite of the fact that are valuable theoretical and practical studies, this kind of analysis has not been used in the previous studies. In fact, there are no limitations in the input dataset, which is a suitable advantage of this approach. Therefore, in the present research work, given the theoretical foundations of the blasting and empirical and mathematical models, and considering the uncertainty and instability of results and consequences of the blasting patterns used in Sungun copper mine and limitations present in the applied models as well as empirical and mathematical approaches, the optimization of blasting pattern and evaluation of the most critical undesired effects of blasting operation in different zones of the Sungun mine were investigated operationally with a viewpoint different from other research works using the abilities and features of the intelligent systems and meta-heuristic algorithms.

As mentioned earlier, ground vibration is one of the most important unpleasant phenomena resulting from the blast that influences all the living and non-living creatures in the surrounding areas. The present study aims to provide a new evaluation system for analyzing and ranking the blasting patterns to determine the most appropriate and optimum blasting pattern from among the designed blasting patterns for the Sungun copper mine in order to reduce the ground vibration phenomenon and its effect on the surrounding area of mine.

In this work, first, using one of the most widely used meta-heuristic algorithms called the imperialist competitive algorithm, different blasting patterns were evaluated and classified based on the data relating to each one. Then, in the next step, the patterns in a cluster with the lowest vibration were ranked. It is worth mentioning that one of the innovations of this study compared to others is the fact that this analysis and evaluation method includes integration of clustering and ranking, which has not been used in other studies yet, and also has practical applications in the executive projects.

## 2. Sungun copper mine

The Sungun copper mine is one of the most important copper mines in Iran and the Middle East, which is located 105 km NE of Tabriz, 75 km NW of Ahar, and 28 km north of Varzaghan in the

vicinity of the Republic of Azerbaijan and the Republic of Armenia. Its longitude is 46 degrees and 43 minutes east and its latitude is 38 degrees and 42 minutes north, and the average height of the region is 2000 m from the sea level (maximum 2700 m), which is located on the global copper belt. This mine is located on the Arasbaran mountain range (Gharadagh) in the form of a penetrated mass. This mountain range with a width of 80 km is a part of the Alpine-Himalayan orogenic belt. The probable reserve of this mine is more than one billion tons, the extractable reserve (given the discoveries made) is about 796 million tons, and the total amount of the definitive, probable and possible reserves in the surrounding area of Varzaghan Sungun mine, is about 1.7 billion tons of copper ore at a grade of 0.61%. Figure 1 shows the location and view of the Sungun copper mine.

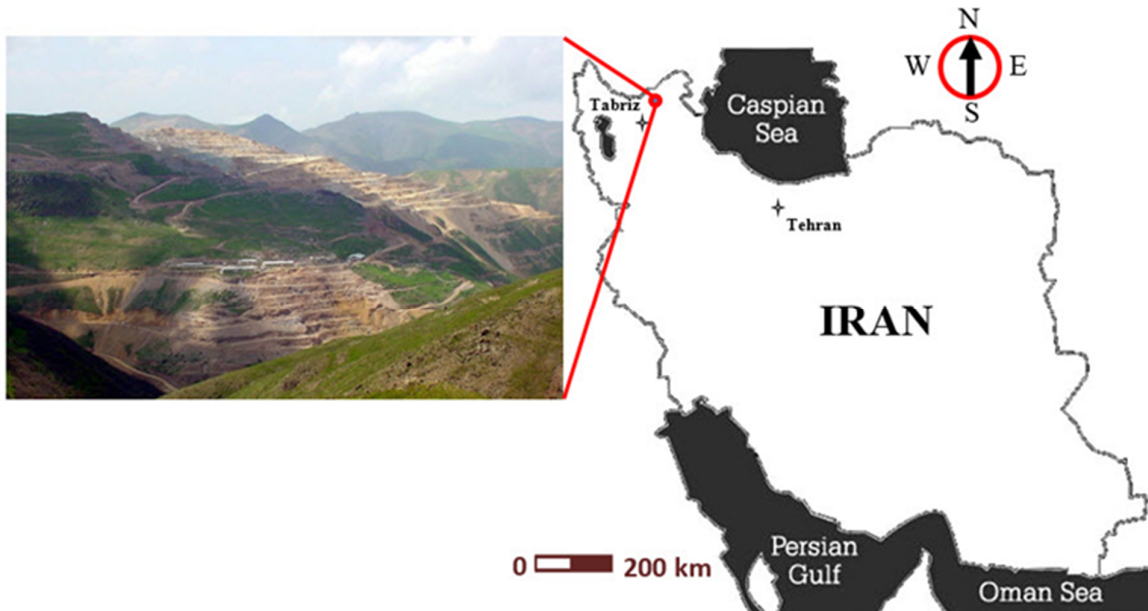


Figure 1. Location of the Sungun copper mine.

### 2.1. Geology and Properties of Studied Area

The Sungun copper deposit is in the northwestern part of a NW-SE trending Cenozoic magmatic belt (Sahand-Bazman), where the porphyry copper deposits are located (Hosseini, and Asghari, 2015). Figure 2 illustrates the geological map of the Sungun copper deposit.

The Sungun porphyry (reportedly Miocene in age, based largely on the regional geological relationships) has intruded a sequence of

Cretaceous limestone and calcareous sedimentary units following collision of the Persian subcontinent with Europe and closure of the Neotethys in the Oligocene–Miocene. The intrusion and the related post-mineralisation dykes are a product of the magmatic activity, the location of which is controlled by the regional fault zones that strike WNW and are compartmentalized by a series of transfer faults that strike NNE-to-NE.

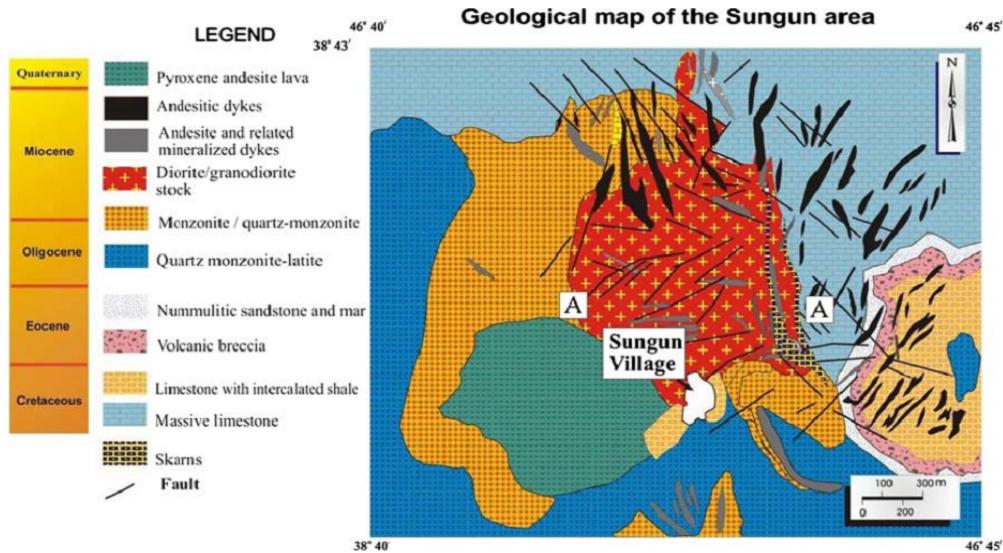


Figure 2. Geological map of the Sungun copper deposit (Hezarkhani, 2006, Hosseini, and Asghari, 2015).

The structure and regional tectonics can be used to constrain the chronology of alteration and mineralisation at Sungun. The following points are suggested:

1. ~20–15 Ma, intrusion of the Sungun porphyry,
2. Propylitic alteration (predominantly meteoric fluids driven by thermal perturbation),
3. Locally developed silica ( $\pm$  kaolinite) acidic alteration as a result of exsolution of magmatic fluids,
4. locally developed sericite + pyrite  $\pm$  quartz alteration, which is fault-controlled and found associated with the WNW, NW, and NE striking faults as well as a number of shallowly west dipping faults,
5. Intrusion of DK1a dykes (possibly synchronously with the sericitic alteration, which is also controlled by locally active faults,
6. 14–10 Ma, quartz + sulphide (including copper) vein mineralisation with a NW preferred orientation,
7. Post-mineralisation, emplacement of NW and WNW striking dykes,
8. < 10 Ma, Late fault movement.

Stages 1 to 5 can be constrained to the period when there was a southwestward shortening as a result of the collision of Persian terranes with Europe. Stages 6 and 7 occurred during southeastward shortening from about 14 Ma as a result of plate reorganisation at that time. Stage 8 may have occurred during several tectonic events in the Pliocene and Quaternary including Quaternary tectomagmatic activity that resulted in the extrusion

of sequences of intermediate tephra and volcanics (NICICo and SRK, 2004).

The properties of the studied area such as rock type, rainfall, intact rock strength (UCS), RQD, tectonic regime, groundwater conditions, number of major discontinuity sets, discontinuity persistence, discontinuity spacing, discontinuity aperture, discontinuity roughness, and discontinuity filling based on geotechnical and field studies are given in Table 1.

Table 1. Properties of the studied area.

Parameters	SW Sungun
Rock type (Major)	Trachyte
Rainfall (mm/year)	300-450
Intact rock strength-UCS (Mpa)	30-80
RQD (%)	50-75
Tectonic regime	Strong
Groundwater conditions	Damp
Number of major discontinuity sets	1
Discontinuity persistence (m)	10-30
Discontinuity spacing (m)	0.06-2
Discontinuity aperture (mm)	0.5-1
Discontinuity roughness (JRC)	Smooth
Discontinuity filling	Hard filling

## 2.2. Blasting Cycle and Environmental Impacts in Sungun Copper Mine

Blasting is the process of reducing a rock to its fragments using an explosive. The conventional blasting operations include drilling holes, charge and detonator in each hole, detonating the charge, and clearing away the broken rock. Figure 3 shows the drilling and blasting cycle (a: drilling, b: charging with explosive, c: checking and measuring the data, d: post-blast assessment) and field data collection on one of the studied benches in the Sungun copper mine.



**Figure 3. Blasting cycle and measuring the field data**

For performing the drilling operations, drilling carriage with deep hammer is intended for drilling diameters of 15–16.5 cm. In order to conduct the analyses, first, before the blasting operations, the geometrical properties (including hole diameter, spacing, burden, and number of holes), and the amount of ammonium nitrate fuel oil (ANFO) were measured and recorded for 45 blasting patterns. All the samples for the previous 45 blasting patterns are shown in Table 2.

It is worth mentioning that all the patterns have the same delay pattern and type of rock. In this case, the type of rock is Trachyte that is an igneous

volcanic rock with an aphanitic to porphyritic texture and the major mineral component of trachyte consists of alkali feldspar.

Then after the blasting operations, the qualitative description of ground vibration resulted from each pattern is evaluated based on Table 2 by the experts in the buildings and facilities around the mine. The ground vibration levels including extremely high, very high, high, fair, low, and very low vibrations are described in Table 2. The qualitative descriptions of the blast results for each pattern are given in Table 3.

**Table 2. Geometrical properties and values of ANFO for 45 blasting patterns.**

Pattern No.	Hole diameter (cm)	Number of holes	Spacing (m)	Burden (m)	ANFO (Kg)	Pattern No.	Hole diameter (cm)	Number of holes	Spacing (m)	Burden (m)	ANFO (Kg)
1	15.24	30	4	3	4170	24	16.5	33	4	3	5000
2	16.5	19	4	3	2420	25	16.5	37	4	3	5050
3	16.5	19	4	3	2000	26	16.5	31	4	3	4550
4	16.5	22	4	3	1500	27	16.5	13	4	3	1100
5	16.5	25	4	3	3480	28	16.5	25	4	3	3450
6	16.5	31	4	3	3670	29	16.5	20	4	3	1950
7	16.5	31	4	3	3200	30	16.5	19	4	3	2000
8	16.5	32	4	3	1650	31	16.5	14	4	3	1500
9	16.5	28	4	3	3080	32	16.5	23	4	3	2160
10	16.5	36	4	3	4500	33	16.5	56	4	3	5250
11	16.5	35	4	3	1600	34	16.5	24	4	3	1800
12	16.5	24	4	3	2560	35	15.24	20	4	3	1050
13	16.5	31	4	3	2020	36	16.5	20	4	3	1450
14	15.24	31	5	4	3750	37	16.5	37	4	3	3000
15	16.5	22	5	4	4420	38	16.5	13	4	3	1530
16	16.5	39	4	3	3620	39	16.5	25	4	3	1870
17	16.5	14	4	3	1860	40	16.5	53	4	3	5650
18	16.5	26	4	3	1300	41	16.5	28	4	3	2800
19	16.5	39	4	3	4900	42	16.5	31	4	3	3470
20	16.5	39	4	3	2600	43	16.5	21	4	3	3300
21	16.5	16	4	3	1790	44	16.5	25	4	3	3200
22	16.5	36	6	5	4900	45	16.5	33	4	3	4200
23	16.5	21	4	3	2700						

**Table 2. Ground vibration levels.**

Ground vibration level	Description
Very low	Detected only by seismograph
Low	Hanging objects may slow swing
Fair	Hanging object swing
High	Damage to weak structures–Thin cracks on wall or roof
Very high	Damage to well-built structures–Cracks in the earth
Extremely high	Destruction and overturning of structures

**Table 3: Qualitative description of blast results for each pattern.**

Patterns No.	Ground vibration (actual)	Pattern No.	Ground vibration (actual)	Pattern No.	Ground vibration (vctual)
1	High	16	High	31	Fair
2	Fair	17	Fair	32	Fair
3	Fair	18	Low	33	Very high
4	Fair	19	High	34	Fair
5	High	20	High	35	Low
6	High	21	Fair	36	Low
7	High	22	Very high	37	High
8	Fair	23	Fair	38	Fair
9	High	24	High	39	Fair
10	High	25	High	40	Very high
11	Fair	26	High	41	High
12	Fair	27	Low	42	High
13	Fair	28	High	43	High
14	High	29	Fair	44	High
15	High	30	Fair	45	High

Considering a high volume of work and various successive blasting operations in this mine, the ground vibration phenomenon happens, which imposes significant damages on the administrative

and technical buildings as well as the surrounding environment. Figure 4 shows samples of damages imposed on the buildings and the surrounding areas of the mine.



**Figure 4. Damages caused by blasting in the (a) structures and (b) environment around of the Sungun copper mine.**

**3. Clustering of Blasting Patterns using Imperialist Competitive Algorithm**

In the recent years, solving complicated and uncertain problems using the algorithms and

optimization methods has increased significantly in all the engineering disciplines, which not only has helped solving these complicated problems but also has innovation in dealing with these problems in

contrast to other classic methods (Salemi et al., 2018; Mikaeil et al., 2018; Aryfar et al., 2018). There are also other studies that show the performance of meta-heuristic algorithms in engineering problems. (Dormishi et al., 2019; Hosseini et al., 2019; Haghshenas et al., 2019; Faradonbeh et al., 2019; Noori et al., 2019).

The imperialist competitive algorithm is one of the meta-heuristic algorithms with a high ability in optimizing and solving complicated problems. In contrast to other evolutionary methods attempting to find an optimum answer for the optimization problems by modeling the natural evolution process, the imperialist competitive algorithm is inspired by a social-political phenomenon. This algorithm has been provided by Atashpaz-Gargari and Lucas (2007) and is generally used in any type of optimization problem without any limitation, and therefore, it has many applications in a wide range of engineering fields. Assimilation policy, imperialist competition, and revolution are three important principles in this algorithm. In this algorithm, each country is considered as a population, and the algorithm is initiated by producing a random population (country). Totally, the population (countries) is divided into imperialists and colonies. In fact, each member that has the lowest expenses according to the optimization function is considered as the imperialist and other populations that impose higher expenses are considered as colonies. Then, in the first step, the normalization expense must be determined for each imperialist based on Equation 1.

$$C_n = c_n - \max_i \{c_i\} \quad (1)$$

where  $C_n$  is the expense of the  $n$ th imperialist,  $\max \{c_i\}$  is the highest expense among the imperialists, and  $c_n$  is the normalized expense of the imperialists. Then, in the next step, according to Equation 2, the relative normalized power of each imperialist is determined for each imperialist based on the normalized expense, and the colonial countries are divided among imperialists based on this power. Figure 5 shows the formation of the initial empires.

$$P_n = \left| \frac{C_n}{\sum_{i=1}^{N_{imp}} C_i} \right| \quad (2)$$

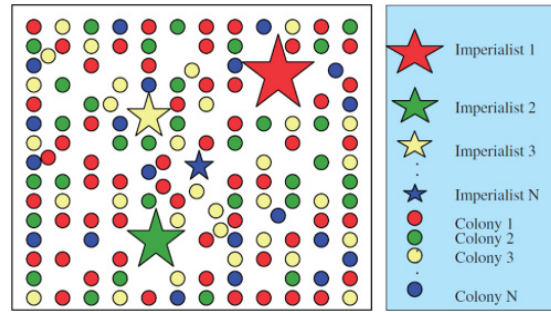


Figure 5. Forming initial imperialists and colonies (Atashpaz-Gargari and Lucas 2007).

Thus the initial number of colonies belonging to one imperialist is determined according to Equation 3, where  $N.C_n$  and  $N_{col}$  are the initial number of colonies of one empire and the total number of colonial countries in the initial population (initial countries), respectively.

$$N.C_n = \text{round}\{P_n(N_{col})\} \quad (3)$$

The movement of the colonies toward the imperialist is shown in Figure 6.

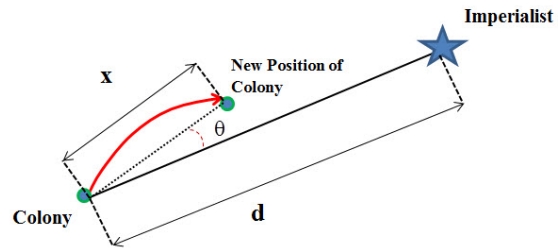


Figure 6. A schematic form of assimilation policy.

$x$  is a random number with a uniform distribution according to Equation 4 and based on Figure 6, and  $d$  is the distance between the imperialist and the colony.  $B$  is a number larger than 1 and close to 2 leading to the vicinity of the colony to the imperialist from different dimensions. Moreover, to increase the searching area around the imperialist, a possible deviation is considered in the path of attracting the colony by the imperialist that occurs in the attraction process. The amount of this angular deviation is equal to  $\theta$ , which follows a uniform distribution based on Equation 5.

$$x \sim U(0, \beta * d) \quad (4)$$

$$\theta \sim U(-\gamma, \gamma) \quad (5)$$

where  $\gamma$  is a parameter that controls the angular deviation range and is equal to  $\frac{\pi}{4}$  based on the empirical results.

The imperialist competition among imperialists is the final step of algorithm, and the total form of this

competition is shown in Figure 7. In this step, the competition among imperialists is initiated and the colonies are attracted toward the stronger imperialist. Finally, the imperialist that loses its

colonies is attracted as a colony by another imperialist. This process is continued until the stop condition of the algorithm is obtained (Atashpaz-Gargari and Lucas 2007).

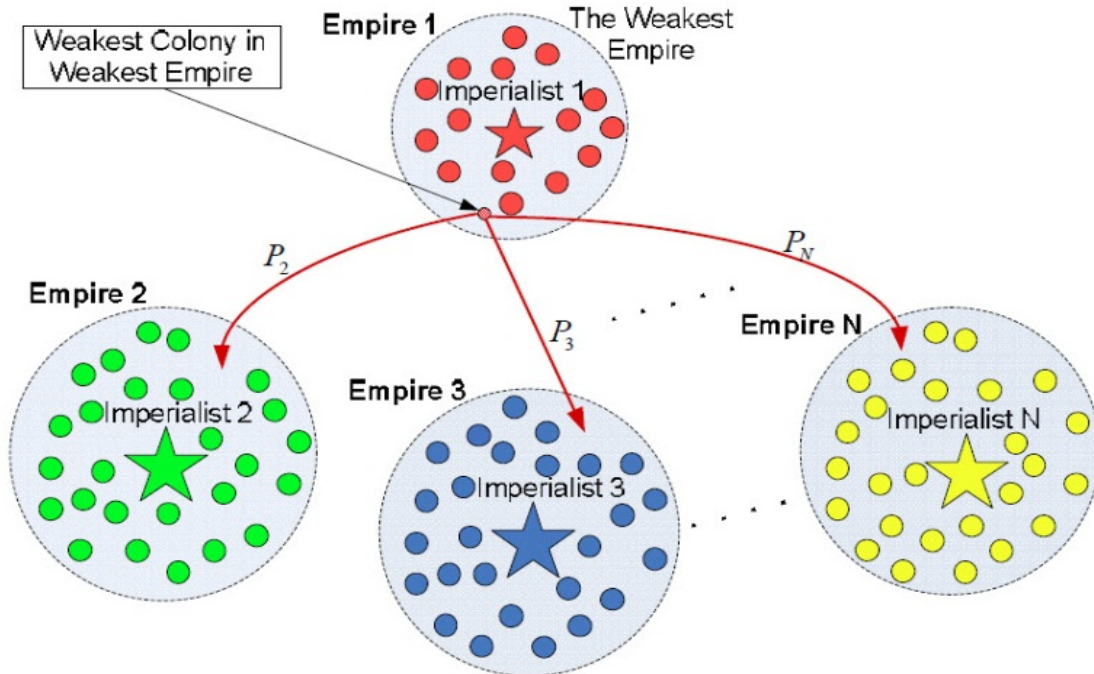


Figure 7. A schematic imperialist competition: the colony of the weakest empire is attracted toward stronger empires (Haghshenas et al., 2017a).

In this step, after collecting the data from each blasting pattern, a developed model is prepared for classifying 45 blasting patterns. The imperialist competitive algorithm is used as a meta-heuristic algorithm to train k-means algorithm in this clustering, in order to determine a developed model, first, the algorithm's control parameters are determined. These parameters play a crucial role in the convergence and enhancement of the algorithm's performance. It is worth noting that since there is no determined relationship between the control parameters, the values for these parameters are determined based on the previous studies and the experts' opinions (Mohammadi et al., 2019; Mikaeil et al., 2019) and the try-and-error methods. For example, 85 or 65 or 55 of populations for modeling were used; in 75 populations, the model had the best performance. Hence, in this model, the values for these control parameters include the maximum iteration of 150, and the minimum acceptance precision of  $\epsilon_L = 0.0001$  and 75 populations as the initial populations for ICA. Therefore, in this modelling, the Lloyd's algorithm (k-means clustering) is used according to Equation 6 as the objective function in the

imperialist competitive algorithm in order to analyze clustering (Lloyd 1982).

$$Obj.Function = \sum_{i=1}^n \min_{1 \leq j \leq k} d(x_i, m_j) \quad (6)$$

where  $x_i$  is the data of a collection and the value of  $i$  is equal to  $i = [1, 2, 3, \dots, n]$ ,  $m_i$  and  $k$  are the centers of each cluster and the number of clusters, respectively, and  $d$  is the Euclidean distance between the center of each cluster and its members. According to the experts' opinions, the blasting patterns could be placed into two acceptable (fair and low) and unacceptable (high and very high) vibration levels with blue and yellow colors, respectively, based on which the desired analyses are done considering the two clusters. In fact, it should be noted that the ground vibrations as the actual observations are considered in 4 labels (fair, low, high, and very high) and two classes in which fair and low belong to an acceptable class, and high and very high belong to unacceptable. Additionally, in the next analyses, the data is classified considering 3 and 4 clusters but the algorithm only classifies the data into two clusters, and finally, all the answers are based on the two-cluster clustering.

It means that according to the algorithm's detection, the data can only be placed in two clusters even if the number of clusters introduced to the algorithm for data analysis is more than two. The results

obtained from the classified analyses and the real samples from the vibration intensity after the blasting operations are shown in Table 4 in order to validate the clustering results.

**Table 4. Optimization results of clustering by the imperialist competitive algorithm with 2 clusters.**

Pattern No.	Optimum partition		Clusters	Ground vibration (actual)	Pattern No.	Optimum partition		Clusters	Ground vibration (actual)
	First class	Second class				First class	Second class		
1	0.447	0.106	2	High	24	0.597	0.221	2	High
2	0.102	0.327	1	Fair	25	0.635	0.249	2	High
3	0.037	0.384	1	Fair	26	0.510	0.140	2	High
4	0.070	0.435	1	Fair	27	0.192	0.575	1	Low
5	0.296	0.128	2	High	28	0.291	0.130	2	High
6	0.370	0.024	2	High	29	0.018	0.381	1	Fair
7	0.300	0.101	2	High	30	0.037	0.384	1	Fair
8	0.207	0.374	1	Fair	31	0.135	0.509	1	Fair
9	0.252	0.137	2	High	32	0.067	0.322	1	Fair
10	0.541	0.154	2	High	33	0.871	0.511	2	Very high
11	0.261	0.388	1	Fair	34	0.062	0.372	1	Fair
12	0.137	0.252	1	Fair	35	0.163	0.527	1	Low
13	0.188	0.308	1	Fair	36	0.074	0.458	1	Low
14	0.468	0.255	2	High	37	0.355	0.168	2	High
15	0.522	0.320	2	High	38	0.148	0.515	1	Fair
16	0.452	0.137	2	High	39	0.078	0.355	1	Fair
17	0.118	0.460	1	Fair	40	0.885	0.509	2	Very high
18	0.139	0.447	1	Low	41	0.212	0.182	2	High
19	0.629	0.242	2	High	42	0.339	0.055	2	High
20	0.353	0.246	2	High	43	0.254	0.205	2	High
21	0.083	0.445	1	Fair	44	0.248	0.154	2	High
22	0.797	0.550	2	Very high	45	0.468	0.083	2	High
23	0.148	0.266	1	Fair					

According to Table 4, for each blasting pattern, the Euclidean distance from the center of each cluster is determined in the columns of optimum partition, and it should be noted that the Euclidean distance is dimensionless. Accordingly, the distance of each blasting pattern from the center of each cluster with the minimum value is the blasting pattern relating to that cluster. For example, in the blasting pattern No. 1, the Euclidean distance from the center of the first cluster is equal to 0.447 and the distance from the center of the second cluster is equal to 0.106, and therefore, this blasting pattern is closer to the center of the second cluster. Thus it belongs to the second cluster. In another example, the Euclidean distance between the center of the first cluster and the second blasting pattern is equal to 0.102, which is less than the Euclidean distance of this pattern from the center of the second cluster, i.e. equal to 0.327. Thus the second blasting pattern belongs to the second cluster. Therefore, according to the analyses conducted by the proposed model, the belonging of each blasting pattern to each cluster is determined in the cluster column. On the other hand, the patterns' clustering validation plays an important role in proving the analyses and the

procedure of this process. As a result, in the last column of Table 3, the ground vibration intensity resulting from each blasting pattern is recorded and used for validating the patterns' clustering results. According to the results obtained and their concordance with the results of the vibration resulting from each blasting pattern based on the last column of Table 3, it is determined that the blasting patterns with fair and low vibrations (21 blasting patterns) are placed in the first cluster and the blasting patterns with much and too much vibrations (24 blasting patterns) are placed in the second one. It means that the proposed model could accurately and correctly diagnose the blasting patterns with acceptable (fair and low) vibration levels according to the geometrical properties and the amount of ANFO in each blasting pattern from among the unacceptable (high and very high) vibrations. It is worth mentioning that the control parameters considered by the experts in this model lead to the high convergence of the algorithm in reaching an optimum answer with a high accuracy and precision.

**4. Ranking of Patterns using TOPSIS Technique**

Complexity of the decision-making and planning environment, too much data, and uncertainty have led to the application of multi-attribute decision-making techniques because having a one-dimensional view toward these kinds of problems does not lead to accurate and precise answers. The Technique for the Order Performance by Similarity to Ideal Solution (TOPSIS) method is a ranking method in the multi-attribute decision making (MADM) problems, provided by Hwang and Yoon (1981), and due to its high flexibility and ability in matching the opinion of experts with the problem's data, it has numerous applications in the engineering and administration fields. In this method, not only the distance of each option from the ideal solution is considered but also the distance of each option from the negative ideal solution is studied, and generally, the selected option must have the least Euclidean distance from the ideal solution and the maximum Euclidean distance from the negative ideal solution. The TOPSIS ranking method with n criteria and m option provided in this study is as follows:

Step 1: Formation of decision matrix is the first step in this method, which according to matrix A, is formed as follows:

$$A = \begin{pmatrix} X_{11} & X_{12} & \dots & X_{1n} \\ X_{21} & X_{22} & \dots & X_{2n} \\ \vdots & \vdots & \ddots & \vdots \\ X_{m1} & X_{m2} & \dots & X_{mn} \end{pmatrix}$$

where  $X_{mn}$  is the performance of option i (i = 1,2,3,...,m) in relation to the criterion j (j = 1,2,3,...,n).

Step 2: In this step, the decision matrix is descaled in order to turn the criteria with different dimensions into dimensionless criteria, and the resulting matrix is defined according to matrix R as follows:

$$R = \begin{pmatrix} r_{11} & r_{12} & \dots & r_{1n} \\ r_{21} & r_{22} & \dots & r_{2n} \\ \vdots & \vdots & \ddots & \vdots \\ r_{m1} & r_{m2} & \dots & r_{mn} \end{pmatrix}$$

Additionally, Equation 6 is used for descaling in this step.

$$r_{ij} = \frac{x_{ij}}{\sqrt{\sum_{i=1}^m x_{ij}^2}} \tag{7}$$

Step 3: In this step, the standard weight vector is formed based on different standard significance coefficients in the decision-making, and is defined based on  $W = [w_1, w_2, \dots, w_n]$ , where  $w_i$  (i=1,2,...,n) is the standard weight.

Step 4: After determining the weight vector in the previous step, by multiplying this vector by the descaled decision matrix, a descaled weighted matrix is obtained; each of its arrays is according to Equation 8.

$$v_{ij} = w_j r_{ij} \quad j = 1, \dots, n; i = 1, \dots, m. \tag{8}$$

Step 5: The positive ideal solution with symbol  $A^*$  and the negative ideal solution with symbol  $A^-$  are obtained from Eqs. 9 and 10, respectively, where  $v_j^*$  and  $v_j^-$  indicate the best and worst values of criterion j from among other options, respectively.

$$A^* = \{v_1^*, v_2^*, \dots, v_j^*, \dots, v_n^*\} \tag{9}$$

$$A^- = \{v_1^-, v_2^-, \dots, v_j^-, \dots, v_n^-\} \tag{10}$$

Step 6: In this step, first, the distance of each option from the positive ideal and negative ideal solutions is calculated according to Eqs. 11 and 12, and then the closeness index for each option is calculated according to the distances obtained from Equation 13, where the indices i and j are the criterion and option, respectively. By comparing  $C_i$  values, the ranking of alternatives is determined.

$$S_i^* = \sqrt{\sum_{j=1}^n (v_{ij} - v_j^*)^2} \tag{11}$$

$$S_i^- = \sqrt{\sum_{j=1}^n (v_{ij} - v_j^-)^2} \tag{12}$$

$$C_i = \frac{S_i^-}{S_i^* + S_i^-} \tag{13}$$

In this step, by having the data separated based on the ICA clustering method, ranking is done for each one of the clusters. By ranking the data of the first cluster (patterns with low and fair vibrations) and data of the second cluster (patterns with high and very high vibrations), the most suitable and the least suitable blasting patterns were determined, respectively. It means that first, the decision matrix is separately formed for the data of each cluster, and then they are descaled based on Equation 7. Tables

5 and 6 show the decision matrices for the first and second clusters, respectively. The evaluation criteria in this clustering from C1 to C5 include the hole diameter, number of holes, spacing, burden,

and ANFO, respectively. Tables 7 and 8 show the normalized decision matrix for the blasting patterns of clusters 1 and 2, respectively.

**Table 5. Decision matrix for the first cluster.**

Pattern No.	Hole diameter (C1)	Number of holes (C2)	Spacing (C3)	Burden (C4)	ANFO (C5)
2	16.5	19	4	3	2420
3	16.5	19	4	3	2000
4	16.5	22	4	3	1500
8	16.5	32	4	3	1650
11	16.5	35	4	3	1600
12	16.5	24	4	3	2560
13	16.5	31	4	3	2020
17	16.5	14	4	3	1860
18	16.5	26	4	3	1300
21	16.5	16	4	3	1790
23	16.5	21	4	3	2700
27	16.5	13	4	3	1100
29	16.5	20	4	3	1950
30	16.5	19	4	3	2000
31	16.5	14	4	3	1500
32	16.5	23	4	3	2160
34	16.5	24	4	3	1800
35	15.24	20	4	3	1050
36	16.5	20	4	3	1450
38	16.5	13	4	3	1530
39	16.5	25	4	3	1870

**Table 6. Decision matrix for the second cluster.**

Pattern No.	Hole diameter (C1)	Number of holes (C2)	Spacing (C3)	Burden (C4)	ANFO (C5)
1	15.24	30	4	3	4170
5	16.5	25	4	3	3480
6	16.5	31	4	3	3670
7	16.5	31	4	3	3200
9	16.5	28	4	3	3080
10	16.5	36	4	3	4500
14	15.24	31	5	4	3750
15	16.5	22	5	4	4420
16	16.5	39	4	3	3620
19	16.5	39	4	3	4900
20	16.5	39	4	3	2600
22	16.5	36	6	5	4900
24	16.5	33	4	3	5000
25	16.5	37	4	3	5050
26	16.5	31	4	3	4550
28	16.5	25	4	3	3450
33	16.5	56	4	3	5250
37	16.5	37	4	3	3000
40	16.5	53	4	3	5650
41	16.5	28	4	3	2800
42	16.5	31	4	3	3470
43	16.5	21	4	3	3300
44	16.5	25	4	3	3200
45	16.5	33	4	3	4200

**Table 7. Normalized decision matrix for the first cluster.**

Pattern No.	Hole diameter (C1)	Number of holes (C2)	Spacing (C3)	Burden (C4)	ANFO (C5)
2	0.219	0.186	0.218	0.218	0.285
3	0.219	0.186	0.218	0.218	0.236
4	0.219	0.216	0.218	0.218	0.177
8	0.219	0.314	0.218	0.218	0.195
11	0.219	0.343	0.218	0.218	0.189
12	0.219	0.235	0.218	0.218	0.302
13	0.219	0.304	0.218	0.218	0.238
17	0.219	0.137	0.218	0.218	0.219
18	0.219	0.255	0.218	0.218	0.153
21	0.219	0.157	0.218	0.218	0.211
23	0.219	0.206	0.218	0.218	0.318
27	0.219	0.128	0.218	0.218	0.130
29	0.219	0.196	0.218	0.218	0.230
30	0.219	0.186	0.218	0.218	0.236
31	0.219	0.137	0.218	0.218	0.177
32	0.219	0.226	0.218	0.218	0.255
34	0.219	0.235	0.218	0.218	0.212
35	0.202	0.196	0.218	0.218	0.124
36	0.219	0.196	0.218	0.218	0.171
38	0.219	0.128	0.218	0.218	0.180
39	0.219	0.245	0.218	0.218	0.221

**Table 8. Normalized decision matrix for the second cluster.**

Pattern No.	Hole diameter (C1)	Number of holes (C2)	Spacing (C3)	Burden (C4)	ANFO (C5)
1	0.190	0.179	0.195	0.191	0.210
5	0.205	0.149	0.195	0.191	0.175
6	0.205	0.185	0.195	0.191	0.185
7	0.205	0.185	0.195	0.191	0.161
9	0.205	0.167	0.195	0.191	0.155
10	0.205	0.215	0.195	0.191	0.227
14	0.190	0.185	0.243	0.255	0.189
15	0.205	0.131	0.243	0.255	0.222
16	0.205	0.233	0.195	0.191	0.182
19	0.205	0.233	0.195	0.191	0.247
20	0.205	0.233	0.195	0.191	0.131
22	0.205	0.215	0.292	0.319	0.247
24	0.205	0.197	0.195	0.191	0.252
25	0.205	0.221	0.195	0.191	0.254
26	0.205	0.185	0.195	0.191	0.229
28	0.205	0.149	0.195	0.191	0.174
33	0.205	0.334	0.195	0.191	0.264
37	0.205	0.221	0.195	0.191	0.151
40	0.205	0.316	0.195	0.191	0.284
41	0.205	0.167	0.195	0.191	0.141
42	0.205	0.185	0.195	0.191	0.175
43	0.205	0.125	0.195	0.191	0.166
44	0.205	0.149	0.195	0.191	0.161
45	0.205	0.197	0.195	0.191	0.211

In the next step, the weights of the criteria were determined by a professional group of experts including 10 experts; they were equal to 0.3, 0.1, 0.12, 0.12, and 0.36 for C1-C5, respectively. Accordingly, the ANFO value has the highest impact on the blasting process compared to four geometrical properties, and the number of holes has the lowest impact on this process compared to the other geometrical properties. However, it is worth mentioning that these criteria are considered as

negative ones in the first cluster ranking to determine the most suitable blasting pattern with the lowest vibration because by increasing each of them, the vibration intensity is also increased, while these criteria are considered as positive in the blasting patterns with much and too much vibrations because the purpose of this ranking is to determine the least suitable blasting pattern with the highest amount of vibration. According to the explanations and Equations 8 to 10, the descaled

weighted decision matrix is formed for clusters 1 and 2, and the positive ideal and negative ideal values are obtained as follows.

- Positive ideal and negative ideal solutions for the first data cluster:

$$A^* = \{0.061, 0.013, 0.026, 0.026, 0.045\}$$

$$A^- = \{0.066, 0.034, 0.026, 0.026, 0.115\}$$

- Positive ideal and negative ideal solutions for the second data clusters:

$$A^* = \{0.062, 0.033, 0.035, 0.038, 0.102\}$$

$$A^- = \{0.057, 0.013, 0.023, 0.023, 0.047\}$$

In the final step, according to Equations 11 to 13, distance from the positive ideal solutions, negative ideals, and the closeness index are determined for each one of the blasting patterns, respectively. The results obtained from this analysis and ranking of clusters 1 and 2 are determined in Tables 9 and 10, respectively.

**Table 9. Results of ranking for the first cluster.**

Pattern No.	Distance of positive ideal solution	Distance of negative ideal Ss	Closeness coefficient	Ranking	Ground vibration (actual)
2	0.059	0.020	0.251	18	Fair
3	0.041	0.034	0.450	15	Fair
4	0.022	0.053	0.708	7	Fair
8	0.032	0.045	0.583	9	Fair
11	0.032	0.047	0.592	8	Fair
12	0.065	0.012	0.159	20	Fair
13	0.045	0.029	0.393	16	Fair
17	0.035	0.041	0.542	11	Fair
18	0.017	0.060	0.776	3	Low
21	0.032	0.043	0.573	10	Fair
23	0.071	0.014	0.163	19	Fair
27	0.005	0.071	0.929	1	Low
29	0.039	0.035	0.473	14	Fair
30	0.041	0.034	0.450	15	Fair
31	0.020	0.055	0.735	5	Fair
32	0.048	0.026	0.347	17	Fair
34	0.034	0.040	0.539	12	Fair
35	0.007	0.072	0.913	2	Low
36	0.019	0.055	0.743	4	Low
38	0.021	0.054	0.721	6	Fair
39	0.037	0.037	0.496	13	Fair

**Table 10. Results of ranking for the second cluster.**

Pattern No.	Distance of positive ideal solution	Distance of negative ideal Ss	Closeness coefficient	Ranking	Groundv (actual)
1	0.037	0.029	0.440	11	High
5	0.048	0.017	0.261	16	High
6	0.043	0.021	0.325	14	High
7	0.051	0.013	0.208	19	High
9	0.053	0.011	0.168	22	High
10	0.031	0.036	0.538	7	High
14	0.039	0.024	0.378	12	High
15	0.032	0.035	0.523	9	High
16	0.043	0.022	0.339	13	High
19	0.026	0.043	0.628	5	High
20	0.059	0.012	0.165	23	High
22	0.018	0.047	0.722	2	Very high
24	0.026	0.044	0.627	6	High
25	0.025	0.046	0.648	4	High
26	0.031	0.036	0.535	8	High
28	0.048	0.016	0.253	17	High
33	0.021	0.053	0.719	3	Very high
37	0.053	0.013	0.196	20	High
40	0.019	0.059	0.752	1	Very high
41	0.058	0.007	0.112	24	High
42	0.046	0.018	0.274	15	High
43	0.051	0.014	0.209	18	High
44	0.052	0.012	0.189	21	High
45	0.035	0.030	0.461	10	High

According to Table 7, ranking for the blasting patterns was done in two different clusters; based on the closeness index, the blasting pattern No. 27 with the specification including the hole diameter = 16.5 (cm), number of holes = 13, spacing= 4 (m), burden= 3 (m), and ANFO = 1100 (Kg) has the highest closeness index being equal to 0.929, i.e. this blasting pattern has the lowest amount of vibration and could obtain the first rank in the TOPSIS technique. On the other hand, this ranking has a very precise match with the ground vibration observed in each blasting pattern, which has been determined in the last column of this table in order to validate the clustering results. It shows the accuracy of the ranking and procedure considered for studying and evaluating the vibration amount of different blasting patterns. On the other hand, according to the ranking results in Table 8, the blasting pattern No. 40 with specifications of the hole diameter = 16.5 (cm), number of holes = 53, spacing = 4 (m), burden = 3 (m), and ANFO = 5650 (Kg) has the highest closeness index being equal to 0.752, showing that this blasting pattern has the maximum ground vibration, which could impose significant damages on the buildings and facilities in the area around the mine, and according to the TOPSIS ranking method, it receives the first rank among the blasting patterns with unpleasant vibrations. In addition, the following remarks could be extracted from the results obtained.

- ANFO is the most influential criterion in a blasting pattern, which could play a significant role in the amount of ground vibration, while the number of holes in a blasting pattern had the minimum impact on producing the ground vibration compared to the other criteria.
- According to the control parameters considered for ICA for training the k-means algorithm by the professional experts, based on the previous studies and try-and-error methods and also according to the criteria measured in each blasting pattern, the proposed model had a very suitable accuracy and precision and could accurately classify and separate the blasting patterns into acceptable (fair and low) and dangerous (high and very high) vibration levels, and the results of this clustering were completely matched with the results of the observed ground vibrations.
- According to the influential criteria and the ranking, the blasting pattern No. 27 was selected as a pattern with the least amount of vibration, which had a suitable match in the blasting process. Therefore, this pattern is suggested to be used in the extraction unit of the Sungun copper mine currently under operation and some

parts of this mine that are going to be exploited in the future.

Consequently, it could be said that this new approach for evaluating and selecting a suitable blasting pattern, i.e. using the clustering method with ranking into MCDM methods, is a practical method in reducing the ground vibration and the damages imposed on the buildings and the mine's surrounding environment. On the other hand, it must be emphasized that the results and analyses are introductory and preliminary, and for using this approach in the evaluation and selection of a suitable blasting pattern in other open-pit mining operations with different conditions, specification, and stone diversity, more studies and analyses must be carried out to verify this approach.

## 5. Conclusions

The blasting operation is one of the most widely used extraction methods in the open-pit mines, which is preferred over many extraction methods in most countries due to its numerous advantages such as high speed and low expenses. However, despite its advantages, this method has many disadvantages, the most important of which is the ground vibration, which not only imposes damages on the nearby structures but also causes damages in the area around the mine. Therefore, the study and selection of a blasting pattern with the minimum amount of damages under the ground vibration plays a crucial role in the maintenance and safety of the environment and the buildings around the mine. In this work, by providing a new evaluation system for studying and selecting the best blasting pattern, 45 blasting patterns in the Sungun copper mine were investigated. Although some studies were conducted to determine the most suitable blasting pattern, the application of a clustering and then ranking method based on the MCDM methods in the process of data analysis is one of the most important innovation reasons in this process. Finally, according to the results obtained from 45 blasting patterns, 21 patterns were placed in the clusters with low and fair vibrations, and the rest were placed in a cluster with high and very high vibrations. Furthermore, in the next step of the evaluation process, the data classified through the TOPSIS method was ranked. The ranking results showed that the blasting pattern No. 27 with specifications of the hole diameter = 16.5 (cm), number of holes = 13, spacing = 4 (m), burden = 3 (m), and ANFO = 1100 (Kg) could be a proper pattern in the rest of the operations of this mine, and also it could be used as a suggestion for new sections of the mine that are going to be exploited

in the next years. Finally, it is recommended to study and evaluate the application of this approach, i.e. the clustering and ranking of blasting patterns, in other open-pit mining operations with other clustering algorithms and decision-making methods.

## References

- [1]. Asghari O, Hezarkhani A (2008) Applying discriminant analysis to separate the alteration zones within the Sungun porphyry copper deposit. *J Appl Sci* 8(24):4472–4486.
- [2]. Armaghani, D.J., Momeni, E., Abad, S.V.A.N.K. and Khandelwal, M. (2015). Feasibility of ANFIS model for prediction of ground vibrations resulting from quarry blasting. *Environmental earth sciences*, 74(4), 2845-2860.
- [3]. Armaghani, D.J., Hasanipanah, M., Amnieh, H.B. and Mohamad, E.T. (2018). Feasibility of ICA in approximating ground vibration resulting from mine blasting. *Neural Computing and Applications*, 29(9): 457-465.
- [4]. Aryafar, A., Mikaeil, R., Haghshenas, S.S. and Haghshenas, S.S. (2018). Application of metaheuristic algorithms to optimal clustering of sawing machine vibration. *Measurement*, 124: 20-31.
- [5]. Atashpaz-Gargari, E. and Lucas, C. (2007, September). Imperialist competitive algorithm: an algorithm for optimization inspired by imperialistic competition. In 2007 IEEE congress on evolutionary computation (pp. 4661-4667). IEEE.
- [6]. Arthur, C.K., Temeng, V.A. and Ziggah, Y.Y. (2019). Novel approach to predicting blast-induced ground vibration using Gaussian process regression. *Engineering with Computers*, 1-14. doi: 10.1007/s00366-018-0686-3.
- [7]. Ataei, M. and Baydokhti, H.A. (2019). An experimental study of the repeated blasting effect on surrounding rock weakness incorporating ultrasonic wave velocity measurement. *Rudarsko-geološko-naftni zbornik*, 34 (4).
- [8]. Azimi, Y., Khoshrou, S.H. and Osanloo, M. (2019). Prediction of blast induced ground vibration (BIGV) of quarry mining using hybrid genetic algorithm optimized artificial neural network. *Measurement*, 106874. doi:10.1016/j.measurement.2019.106874.
- [9]. Dehghani, H. and Shafaghi, M. (2017). Prediction of blast-induced flyrock using differential evolution algorithm. *Engineering with Computers* 33 (1): 149-158.
- [10]. Dormishi, A.R., Ataei, M., Khaloo Kakaie, R., Mikaeil, R. and Shaffiee Haghshenas, S. (2019). Performance evaluation of gang saw using hybrid ANFIS-DE and hybrid ANFIS-PSO algorithms. *Journal of Mining and Environment*. 10 (2): 543-557.
- [11]. Faradonbeh, R.S. and Monjezi, M. (2017). Prediction and minimization of blast-induced ground vibration using two robust meta-heuristic algorithms. *Engineering with Computers*. 33 (4): 835-851. doi: 10.1007/s00366-017-0501-6.
- [12]. Faradonbeh, R.S., Haghshenas, S.S., Taheri, A. and Mikaeil, R. (2019). Application of self-organizing map and fuzzy c-mean techniques for rockburst clustering in deep underground projects. *Neural Computing and Applications*, 1-15. doi:10.1007/s00521-019-04353-z
- [13]. Fouladgar, N., Hasanipanah, M. and Amnieh, H.B. (2017). Application of cuckoo search algorithm to estimate peak particle velocity in mine blasting. *Engineering with Computers*. 33 (2): 181-189.
- [14]. Hasanipanah, M., Monjezi, M., Shahnazar, A., Armaghani, D.J. and Farazmand, A. (2015). Feasibility of indirect determination of blast induced ground vibration based on support vector machine. *Measurement*, 75, 289-297.
- [15]. Hasanipanah, M., Naderi, R., Kashir, J., Noorani, S.A. and Qaleh, A.Z.A. (2017). Prediction of blast-produced ground vibration using particle swarm optimization. *Engineering with Computers*. 33 (2): 173-179.
- [16]. Haghshenas, S.S., Haghshenas, S.S., Mikaeil, R., Sirati Moghadam, P. and Haghshenas, A.S. (2017a). A new model for evaluating the geological risk based on geomechanical properties—case study: the second part of emamzade hashem tunnel. *Electron J Geotech Eng*. 22 (01): 309-320.
- [17]. Haghshenas, S.S., Faradonbeh, R.S., Mikaeil, R., Haghshenas, S.S., Taheri, A., Saghatforoush, A. and Dormishi, A. (2019). A new conventional criterion for the performance evaluation of gang saw machines. *Measurement*, 146, 159-170. doi: 10.1016/j.measurement.2019.06.031.
- [18]. Hezarkhani A (2006) Petrology of the intrusive rocks within the Sungun Porphyry Copper Deposit Azerbaijan, Iran. *J Asian Earth Sci* 27: 326–340.
- [19]. Hosseini, S.A., Asghari, O. Simulation of geometallurgical variables through stepwise conditional transformation in Sungun copper deposit, Iran. *Arab J Geosci* 8, 3821–3831 (2015). doi: 10.1007/s12517-014-1452-5.
- [20]. Hosseini, S.M., Ataei, M., Khalokakaei, R., Mikaeil, R. and Haghshenas, S.S. (2019a). Study of the effect of the cooling and lubricant fluid on the cutting performance of dimension stone through artificial intelligence models. *Engineering Science and Technology, an International Journal*. doi: 10.1016/j.jestch.2019.04.012.
- [21]. Hwang, C.L. and Yoon, K. (1981). Methods for multiple attribute decision making. In *Multiple attribute decision making*. Springer, Berlin, Heidelberg. 186: 58-191. Print ISBN 978-3-540-10558-9. doi: 10.1007/978-3-642-48318-9\_3.

- [22]. Lloyd, S.P. (1982). Least squares quantization in PCM. *IEEE transactions on information theory*, 28(2), 129-137.
- [23]. Monjezi, M., Hasanipanah, M. and Khandelwal, M. (2013). Evaluation and prediction of blast-induced ground vibration at Shur River Dam, Iran, by artificial neural network. *Neural Computing and Applications*, 22(7-8), 1637-1643.
- [24]. Monjezi, M., Baghestani, M., Faradonbeh, R.S., Saghand, M.P. and Armaghani, D.J. (2016). Modification and prediction of blast-induced ground vibrations based on both empirical and computational techniques. *Engineering with Computers*. 32 (4): 717-728.
- [25]. Mohammadi, J., Ataei, M., Kakaie, R., Mikaeil, R. and Haghshenas, S.S. (2019). Performance evaluation of chain saw machines for dimensional stones using feasibility of neural network models. *Journal of Mining and Environment*, 10(4), 1105-1119.
- [26]. Mikaeil, R., Haghshenas, S.S. and Hoseinie, S.H. (2018). Rock penetrability classification using artificial bee colony (ABC) algorithm and self-organizing map. *Geotechnical and Geological Engineering*. 36 (2): 1309-1318.
- [27]. Mikaeil, R., Bakhshinezhad, H., Haghshenas, S.S. and Ataei, M. (2019). Stability Analysis of Tunnel Support Systems Using Numerical and Intelligent Simulations (Case Study: Kouhin Tunnel of Qazvin-Rasht Railway). *Rudarsko-geološko-naftni zbornik*. 34 (2): 1-10. doi: org/10.17794/rgn.2019.2.1.
- [28]. National Iranian Copper Industries Company (NICICo) – Sungun Copper Project (SCP)., S.R.K Consulting, 2004. Structural Geology Model for the Sungun Copper Deposit – NW Iran.
- [29]. Nguyen, H. (2019). Support vector regression approach with different kernel functions for predicting blast-induced ground vibration: a case study in an open-pit coal mine of Vietnam. *SN Applied Sciences*. 1 (4): 283.
- [30]. Nguyen, H. and Bui, X.N. (2019). Predicting blast-induced air overpressure: a robust artificial intelligence system based on artificial neural networks and random forest. *Natural Resources Research*. 28 (3): 893-907.
- [31]. Noori, A.M., Mikaeil, R., Mokhtarian, M., Haghshenas, S.S. and Foroughi, M. (2020). Feasibility of Intelligent Models for Prediction of Utilization Factor of TBM. *Geotechnical and Geological Engineering*, 1-19. doi: 10.1007/s10706-020-01213-9.
- [32]. Norouzi Masir, R., Ataei, M. and Mottahedi, A. (2020). Risk assessment of flyrock in surface mines using FFTA-MCDMs combination. *Journal of Mining and Environment*.
- [33]. Shahnazar, A., Rad, H.N., Hasanipanah, M., Tahir, M.M., Armaghani, D.J. and Ghoroghi, M. (2017). A new developed approach for the prediction of ground vibration using a hybrid PSO-optimized ANFIS-based model. *Environmental earth sciences*. 76 (15): 527.
- [34]. Saghatfroush, A., Monjezi, M., Faradonbeh, R.S. and Armaghani, D.J. (2016). Combination of neural network and ant colony optimization algorithms for prediction and optimization of flyrock and back-break induced by blasting. *Engineering with Computers*. 32 (2): 255-266.
- [35]. Salemi, A., Mikaeil, R. and Haghshenas, S.S. (2018). Integration of finite difference method and genetic algorithm to seismic analysis of circular shallow tunnels (Case study: Tabriz urban railway tunnels). *KSCE Journal of Civil Engineering*. 22 (5): 1978-1990.
- [36]. Shang, Y., Nguyen, H., Bui, X.N., Tran, Q.H. and Moayedi, H. (2019). A Novel Artificial Intelligence Approach to Predict Blast-Induced Ground Vibration in Open-Pit Mines Based on the Firefly Algorithm and Artificial Neural Network. *Natural Resources Research*, 1-15.
- [37]. Singh, T.N. and Singh, V. (2005). An intelligent approach to prediction and control ground vibration in mines. *Geotechnical & Geological Engineering*. 23 (3): 249-262.
- [38]. Yari, M., Bagherpour, R. and Jamali, S. (2017). Development of an evaluation system for blasting patterns to provide efficient production. *Journal of Intelligent Manufacturing*. 28 (4): 975-984.
- [39]. Zhang, X., Nguyen, H., Bui, X.N., Tran, Q. H., Nguyen, D.A., Bui, D.T. and Moayedi, H. (2019). Novel Soft Computing Model for Predicting Blast-Induced Ground Vibration in Open-Pit Mines Based on Particle Swarm Optimization and XGBoost. *Natural Resources Research*, 1-11.

## بررسی و رتبه بندی الگوهای انفجار برای کاهش لرزش زمین با استفاده از روش های محاسبات نرم و تکنیک MCDM

داود محمدی<sup>1</sup>، رضا میکائیل<sup>2\*</sup> و جعفر عبدالهی شریف<sup>3</sup>

- 1- دانشکده مهندسی معدن، واحد اهر، دانشگاه آزاد اسلامی، اهر، ایران
- 2- دانشکده محیط زیست، گروه مهندسی معدن، دانشگاه صنعتی ارومیه، ارومیه، ایران
- 3- دانشکده مهندسی معدن، دانشگاه ارومیه، ارومیه، ایران

ارسال 2020/03/07، پذیرش 2020/05/28

\* نویسنده مسئول مکاتبات: Reza.mikaeil@uut.ac.ir

### چکیده:

روش حفاری و انفجار یکی از روش های مهم استخراج در بیشتر معادن روباز می باشد که به دلیل ارزان بودن و انعطاف پذیری بالا در اجرا، در مقایسه با سایر روش ها از جمله حفر مکانیکی در اولویت قرار دارد. هر چند که در این روش، نباید مشکلات زیست محیطی از قبیل لرزش زمین را نادیده گرفت. از اینرو در این مطالعه به ارائه یک رویکرد نوین در بررسی و انتخاب بهترین الگوی انفجار به منظور کاهش و کنترل لرزش زمین به عنوان یکی از خطرات ناشی از این روش پرداخته می شود. در این بخش از مطالعه 45 الگوی انفجاری از میان الگوهای انفجاری که برای معدن مس سونگون طراحی و مورد استفاده قرار گرفته اند به منظور تعیین مناسب ترین و بهینه ترین الگوی انفجار مورد بررسی و ارزیابی قرار می گیرند. همچنین به دلیل نبود قطعیت نهفته در ماهیت زمین و وجود عدم قطعیت در تحلیل های مربوط به این سیستم حفاری، در این مطالعه در گام اول از تکنیک کلاس بندی به وسیله الگوریتم رقابت استعماری به منظور کلاس بندی داده های جمع آوری شده استفاده شده و در گام دوم برای رتبه بندی نهایی از یکی از روش های تصمیم گیری چند معیاره به نام روش شباهت به گزینه ایده آل استفاده شده است. در نهایت، پس از ارزیابی و رتبه بندی الگوهای مورد مطالعه، الگوی انفجاری شماره 27 انتخاب شد. این الگو می تواند با مشخصات هندسی شامل قطر چال 16/5 سانتی متر، تعداد چال برابر با 13 عدد، فاصله ردیفی 4 متر، بار سنگ 3 متر و خرج مصرفی 1100 کیلوگرم به عنوان مناسب ترین الگوی انفجار با حداقل میزان لرزش و کاهش خسارات به محیط زیست و سازه های ساخته شده در اطراف این معدن مورد استفاده قرار گیرد.

**کلمات کلیدی:** انفجار، لرزش زمین، خوشه بندی، الگوریتم رقابت استعماری، روش شباهت به حل ایده آل.